Spatially Constrained Incoherent Motion (SCIM) model improves quantitative Diffusion-Weighted MRI analysis of Crohn's disease patients

Vahid Taimouri, Moti Freiman, Onur Afacan, and Simon K. Warfield

Computational Radiology Laboratory, Boston Children's Hospital, Harvard Medical School, MA, USA

Abstract. Quantitative analysis of fast and slow diffusion from abdominal Diffusion-weighted MRI has the potential to provide important new insights into physiological and microstructural properties of the body. However, the commonly used, independent voxel-wise fitting of the signal decay model leads to imprecise parameter estimates, which has hampered their practical usage. In this work we evaluated the improvement in the precision of the fast and slow diffusion parameter estimates achieved by using a spatially-constrained Incoherent Motion (SCIM) model of DW-MRI signal decay in 5 healthy subjects and 24 Crohn's disease patients. We found that the improvement in Coefficient of Variation (CV) of the parameter estimates achieved using the SCIM model was significantly larger compared to thus achieved by repeated acquisition and signal averaging (n=5, paired Student's t-test, $p \leq 0.05$). We also found that the SCIM model reduced the coefficient of variation of the parameter estimates of the D^* and f parameter estimates in the ileum by 30% compared to the independent voxel-wise fitting of the signal decay model in the Crohn's patients data (n=24, paired Student's t-test, $p \leq 0.05$). The SCIM model is more precise for quantitative analysis of abdominal DW-MRI signal decay.

1 Introduction

Diffusion-weighted MRI (DW-MRI) of the body is a non-invasive imaging technique sensitive to the incoherent motion of water molecules inside the area of interest. This motion is known to be a combination of a slow diffusion component associated with the Brownian motion of water molecules, and a fast diffusion component associated with the bulk motion of intravascular molecules in the micro-capillaries. These phenomena are characterized through the so-called, intra-voxel incoherent motion (IVIM) model with the slow diffusion (D); the fast diffusion (D^*) as decay rate parameters; and the fractional contribution (f) of each motion to the DW-MRI signal decay [13,14,12].

IVIM model parameters have recently shown promise as quantitative imaging biomarkers for various clinical applications in the body including differential

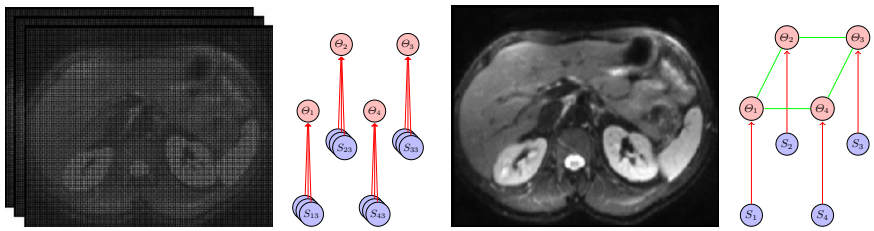

Fig. 1: Illustration of the graphical models used to estimate the fast and slow diffusion parameters from DW-MRI data. (a, b) represents independent voxel-wise estimation of intra-voxel incoherent motion with multiple DW-MRI images averaged, and (c, d) represents voxel-wise estimation of the DW-MRI signal decay model parameters using the spatially constrained incoherent motion model.

analysis of tumors [21,20,11,1,10,15], the assessment of liver cirrhosis [17,19], and Crohn's disease [7].

However, the utility of IVIM parametric imaging with DW-MRI is diminished by a lack of verified methods for producing reliable estimates of both fast and slow diffusion parameters from the DW-MRI signal [12]. Specifically, reliable estimates of IVIM model parameters are difficult to obtain because of 1) the non-linearity of the IVIM model; 2) the limited number of DW-MRI images as compared to the number of the IVIM model parameters, and; 3) the low signal-to-noise ratio (SNR) observed in body DW-MRI.

In current practice, the reliability of the incoherent motion parameter estimates is increased by acquiring multiple DW-MRI images from the patient; next, average these results, and then use the averaged DW-MRI signal to estimate IVIM model parameters. However, this requires substantially increased acquisition times - an undesirable outcome, especially in children, who generally have difficulty in remaining still for long periods of time [12].

Recently, Freiman et al. introduced a new model of DW-MRI signal decay which utilizes the spatial homogeneity as a constraint in the DW-MRI signal decay [8,5]. Essentially, the Spatially Constrained Incoherent Motion (SCIM) model produces estimates of Incoherent Motion model parameters for all voxels simultaneously, rather than solving for each voxel independently. As a result, the reliability of the incoherent motion parameter estimates from the DW-MRI data is increased without acquiring additional data. Fig. 1 depicts the graphical models for the repeated acquisition method used previously to improve parameter estimates reliability (a,b) compared to the SCIM model (c,d).

In this work, we evaluated the improvement in parameter estimates reliability by means of Coefficient of Variation (CV) achieved by using our SCIM model compared to the utilization of the repeated acquisition and signal averaging technique using abdominal DW-MRI data of 5 healthy volunteers. We also compared the CV of fast and slow diffusion parameter estimates obtained form

DW-MRI data of 24 Crohn's disease patients using our SCIM model and the commonly used independent voxel-wise fitting of the IVIM model.

We found that the SCIM model is up to 45% more efficient in improving parameter estimate reliability compared to the repeated acquisition and signal averaging technique (n=5, p≤0.05). We also found that the SCIM model provides 30% improvement in parameter estimates reliability compared to the independent voxel-wise fitting of the IVIM model in DW-MRI data of Crohn's disease patients (p≤0.05).

2 Method

2.1 The Intravoxel incoherent motion model

The Intra-Voxel Incoherent Motion (IVIM) model of DW-MRI signal decay assumes a signal decay function of the form [13,14]:

$$m_{v,i} = s_{0,v}\left(f_v \exp(-b_i(D_v^* + D_v)) + (1 - f_v)\exp(-b_i(D_v))\right) \tag{1}$$

where $m_{i,v}$ is the expected signal of voxel v at b-value=b_i, $s_{0,v}$ is the baseline signal at voxel v; D_v is the slow diffusion decay associated with extravascular water molecules' motion; D_v^* is the fast diffusion decay associated with the intravascular water molecules' motion; and f_v is the fraction between the slow and fast diffusion compartments.

Given the DW-MRI data acquired with multiple b-values, the observed signal (S_v) at each voxel v is a vector of the observed signal at the different b-values: $S_v = \{s_{v,i}\}, i = 1 \ldots N$.

We model the IVIM model parameters at each voxel v as a continuous-valued four-dimensional random variable (i.e. $\Theta_v = \{s_{0,v}, f_v, D_v^*, D_v\}$). Commonly, the IVIM model parameters Θ_v are estimated from the DW-MRI signal S_v using an independent voxel-wise maximum-likelihood estimator:

$$\hat{\Theta_v} = \arg\max_{\Theta_v} p(S_v|\Theta_v) = \prod_{i=1}^{N} p(S_{v,i}|\Theta_v) \tag{2}$$

Using a Gaussian approximation of the non-central χ-distribution of the acquisition noise [4], and taking the negative log of the maximum likelihood estimator; the maximum likelihood estimation takes the form of a least-squares minimization problem:

$$\hat{\Theta}_v = \arg\min_{\Theta_v} \sum_{i=1}^{N} \left(m_{v,i} - s_{v,i}\right)^2 \tag{3}$$

The IVIM model parameters Θ_v are estimated from the DW-MRI signal S_v by solving the least-squares minimization problem (Eq. 3) for each voxel independently using the Levenberg-Marquardt algorithm [16,23]. Initial estimates of the model parameters were obtained with the least squares estimator [9].

2.2 The Spatially Constrained Incoherent Motion (SCIM) model

Taking the Bayesian perspective, our goal is to find the parametric maps Θ that maximize the posterior probability associated with the maps given the observed signal S and the spatial homogeneity prior knowledge:

$$\hat{\Theta} = \arg\max_{\Theta} p(\Theta|S) \propto p(S|\Theta)p(\Theta) \tag{4}$$

Based on the Hammersley-Clifford theorem [22], by using a spatial prior in the form of a continuous-valued Markov random field, the posterior probability $p(S|\Theta)p(\Theta)$ can be decomposed into the product of node and clique potentials:

$$p(S|\Theta)p(\Theta) \propto \prod_{v} p(S_v|\Theta_v) \prod_{v_p \sim v_q} p(\Theta_{v_p}, \Theta_{v_q}) \tag{5}$$

where $p(\Theta_v|S_v)$ is the data term representing the probability of voxel v to have the DW-MRI signal S_v given the model parameters Θ_v, $v_p \sim v_q$ is the collection of the neighboring voxels according to the employed neighborhood system, and $p(\Theta_{v,p}, \Theta_{v,q})$ is the spatial homogeneity prior in the model.

By taking the negative logarithm of the posterior probability (Eq. 5), the maximum a posteriori (MAP) estimate Θ is equivalent to the minimization of:

$$E(\Theta) = \sum_{v} \phi(S_v; \Theta_v) + \sum_{v_p \sim v_q} \psi(\Theta_{v_p}, \Theta_{v_q}) \tag{6}$$

where $\phi(S_v; \Theta_v)$ and $\psi(\Theta_{v,p}, \Theta_{v,q})$ are the compatibility functions:

$$\phi(S_v; \Theta_v) = -\log p(S_v|\Theta_v), \qquad \psi(\Theta_{v_p}, \Theta_{v_q}) = -\log p(\Theta_{v_p}, \Theta_{v_q}) \tag{7}$$

The data term $\phi(S_v; \Theta_v)$ is given by taking the negative logarithm of the likelihood function, the spatial homogeneity term is defined using the robust L1-norm:

$$\psi(\Theta_{v_p}, \Theta_{v_q}) = \alpha W |\Theta_{v_p} - \Theta_{v_q}| \tag{8}$$

where $\alpha \geq 0$ weights the amount of spatial homogeneity enforced by the model, and W is a diagonal weighting matrix that accounts for the different scales of the parameters in Θ_v.

3 Experimental Results

3.1 Precision of incoherent motion parameter estimates from *in-vivo* DW-MRI data of healthy volunteers

We obtained DW-MRI images of 5 health volunteers who underwent research abdominal MRI studies between January 2013 and May 2013. We carried out MR imaging studies of the abdomen using a 1.5-T unit (Magnetom Avanto, Siemens Medical Solutions, Erlangen, Germany) with a body-matrix coil and

a spine array coil for signal reception. Free-breathing single-shot echo-planar imaging was performed using the following parameters: repetition time/echo time (TR/TE) = 6800/59 ms; SPAIR fat suppression; matrix size = 192×156; eld of view = 300×260 mm; number of excitations = 1; slice thickness/gap = 5 mm/0.5 mm; 40 axial slices; 8 b-values = 5,50,100,200,270,400,600,800 s/mm^2. A tetrahedral gradient scheme, first proposed in Conturo et al. [2], was used to acquire 4 successive images at each b-value with an overall scan acquisition time of 4 min. Diffusion trace-weighted images at each b-value were generated using geometric averages of the images acquired in each diffusion sensitization direction [18].

We repeated the imaging acquisition six times to get six DW-MRI datasets, each with low Signal to Noise Ratio (DW-MRI$_{\text{low}}$). We averaged the six DW-MRI datasets to achieve high SNR DW-MRI images (DW-MRI$_{\text{high}}$). We estimated the model parameters from: 1) DW-MRI$_{\text{high}}$ using the independent voxel-wise approach (IVIM$_{\text{high}}$); 2) DW-MRI$_{\text{low}}$ using the independent voxel-wise approach (IVIM$_{\text{low}}$), and 3) DW-MRI$_{\text{low}}$ using the Spatially Constrained Incoherent Motion (SCIM) model (SCIM$_{\text{low}}$).

We calculated the precision of the parameter estimates by means of the coefficient of variation (CV) of the parameter estimates at each voxel in the IVIM and SCIM maps of each patient using model-based wild-bootstrap analysis [3,6]. Fig. 2 depicts a representative parametric maps of the upper abdomen. The SCIM model yields smoother, more realistic maps, especially for the f parameter. We set the value of α to 0.01 and the rescaling matrix W diagonal to $\{1.0, 0.001, 0.0001, 0.01\}$ to provide equal weight to each one of the incoherent motion model parameters. Stopping criteria was defined as an energy improvement of less than 0.1 from the initial energy or 500 iterations.

For each subject, we averaged the CV values over the same, three ROIs mentioned above. We first examined the statistical significance of the difference in the precision of the parameter estimates between the IVIM$_{\text{high}}$ and the IVIM$_{\text{low}}$ estimates using a two-tailed paired Student's t-test with $p \leq .05$ as indicating a significant difference. Then, we examined the statistical significance of the difference in the precision of the parameter estimates between the IVIM$_{\text{low}}$ and the SCIM$_{\text{low}}$ estimates using the same test. We performed the statistical analyses with standard statistical software (Matlab® R2010b; The MathWorks, Natick, MA, USA).

Fig. 3 presents the bar-plots of the CV values for each parameter estmiates. While the repeated acquisition technqiue slightly reduced the CV compared to this of the IVIM$_{\text{low}}$, the difference was not significant. However, by using the SCIM model, the CV of the parameters estimates reduced substantially, by up to 52%. The difference between the CV of the IVIM$_{\text{low}}$ and the SCIM$_{\text{low}}$ was significant. In addition, we found that the SCIM model is up to 45% more efficient in improving parameter estimate reliability compared to the repeated acquisition and signal averaging technique. As seen in Fig. 3, the error bars of IVIM$_{\text{low}}$ are smaller than those of IVIM$_{\text{high}}$, which implies there is less variation with lower SNR. This issue will be investigated more in the future work.

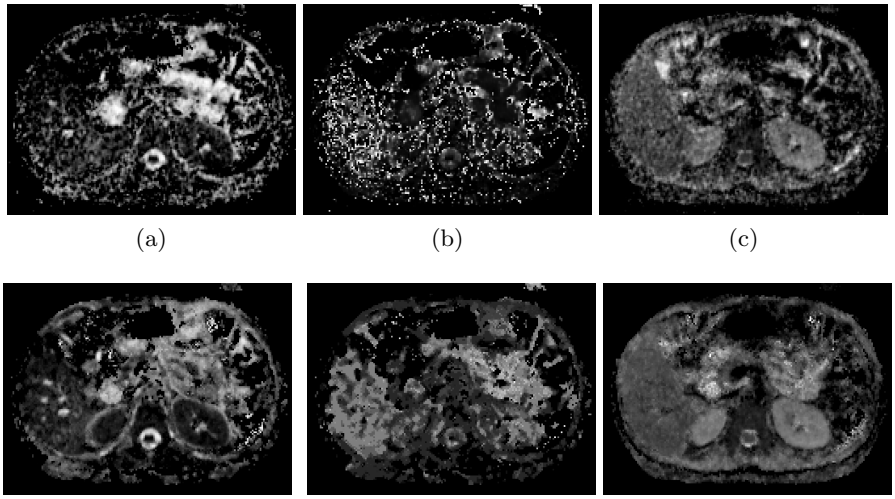

Fig. 2: Representative upper abdomen slice of the parametric maps reconstructed by the IVIM method (1st row), and by the SCIM method (2nd row). The SCIM method yields smoother, more realistic maps, with sensitivity to details.

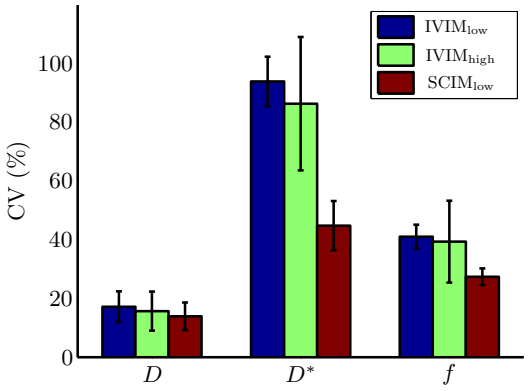

Fig. 3: Bar plot of the CV of the incoherent motion parameters as estimated from 5 healthy subjects. The CV was significantly lower when using our SCIM approach than when using the IVIM approach for all parameters. In contrast, using repeated acquisition and signal averaging did not reduce the coefficient of variation significantly.

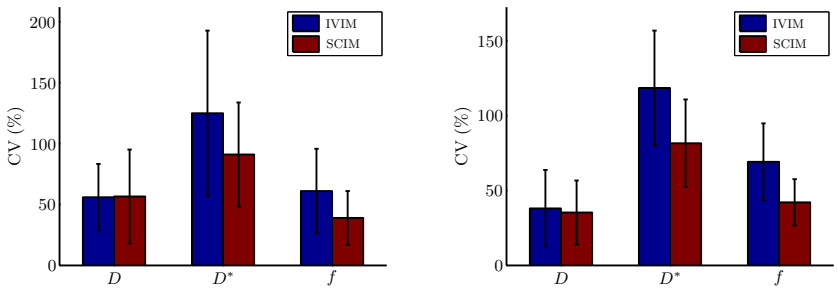

(a) Abormals

Fig. 4: Bar plot of the CV of the incoherent motion parameters as estimated from 24 Crohn's disease subjects (13 with normal ileum and 11 with abnormal findings in the ileum). The CV was significantly lower when using our SCIM approach than when using the IVIM approach for all parameters.

3.2 Precision of incoherent motion parameter estimates from *in-vivo* DW-MRI data of Crohn's disease patients

We acquired DW-MRI and MR enterography (MRE) data from 24 consecutive patients with confirmed Crohn's disease (15 males, 9 females; mean age 14.7 years; range: 5-24 years), who underwent a clinically indicated MRI study between January 1, 2011 and October 31, 2011 in our outpatient MRI department. We carried out MRI imaging studies of the abdomen and the pelvic using a similar protocol to this described in Section 3.1. MR enterography (MRE) protocol for these patients included polyethylene glycol administration for bowel distention and gadolinium-enhanced, dynamic 3D VIBE (volume- interpolated breath hold exam) in the coronal plane.

According to a consensus reading of two board certified radiologists of the MRE data, we classified each patient ileum qualitatively as enhancing or non-enhancing. 11 (46%) patients were diagnosed with abnormal findings in the ileum and in 13 (54%) patients were diagnosed with normal findings in the ileum. We estimated the signal decay model parameters using the IVIM and SCIM models. We calculated the CV of the parameter estimates for each model. Fig. 4 presents the bar-plots of the CV values for each parameter estimates in the ileum for the normal and abnormal groups. The SCIM model reduced the CV of the f and D^* parameters by 36% and 28% for the normal group, and by 39% and 31% for the abnormal group, respectively, compared to the independent voxel-wise fitting of the signal decay model.

4 Conclusions

The role of incoherent motion parameters as quantitative imaging biomarkers for various clinical applications is becoming increasingly important. However, the current method for estimating the DW-MRI signal decay model are not reliable enough. The reliability of the parameter estimates can be improved substantially by using a spatially constrained model for the signal decay model parameter estimation. In this work, we evaluated the improvement achieved by using our SCIM model using *in-vivo* abdominal DW-MRI data of 5 healthy subjects and 24 Crohn's disease patients. The SCIM model provides a better mechanism to estimate the signal decay model parameters and a more precise insight to the physiological causes of the DW-MRI signal decay and then the voxel-wise independent IVIM model.

References

1. Chandarana, H., Lee, V.S., Hecht, E., Taouli, B., Sigmund, E.E.: Comparison of biexponential and monoexponential model of diffusion weighted imaging in evaluation of renal lesions: preliminary experience. Invest Radiol 46(5), 285–91 (2011)
2. Conturo, T.E., McKinstry, R.C., Akbudak, E., Robinson, B.H.: Encoding of anisotropic diffusion with tetrahedral gradients: a general mathematical diffusion formalism and experimental results. Magn Reson Med 35(3), 399–412 (1996)
3. Davidson, R., Flachaire, E.: The wild bootstrap, tamed at last. Journal of Econometrics 146(1), 162 – 169 (2008)
4. Dietrich, O., Raya, J.G., Reeder, S.B., Ingrisch, M., Reiser, M.F., Schoenberg, S.O.: Influence of multichannel combination, parallel imaging and other reconstruction techniques on MRI noise characteristics. Magn Reson Imaging 26(6), 754–62 (2008)
5. Freiman, M., Voss, S., Mulkern, R., Perez-Rossello, J., Callahan, M., Warfield, S.: Reliable Assessment of Perfusivity and Diffusivity from Diffusion Imaging of the Body. In: Ayache, N., Delingette, H., Golland, P., Mori, K. (eds.) Medical Image Computing and Computer-Assisted Intervention MICCAI 2012, Lecture Notes in Computer Science, vol. 7510, pp. 1–9. Springer Berlin / Heidelberg (2012)
6. Freiman, M., Voss, S., Mulkern, R., Perez-Rossello, J., Warfield, S.: Quantitative Body DW-MRI Biomarkers Uncertainty Estimation Using Unscented Wild-Bootstrap. In: Fichtinger, G., Martel, A., Peters, T. (eds.) Medical Image Computing and Computer-Assisted Intervention MICCAI 2011, Lecture Notes in Computer Science, vol. 6892, pp. 74–81. Springer Berlin / Heidelberg (2011)
7. Freiman, M., Perez-Rossello, J.M., Callahan, M.J., Bittman, M., Mulkern, R.V., Bousvaros, A., Warfield, S.K.: Characterization of fast and slow diffusion from diffusion-weighted MRI of pediatric Crohn's disease. J Magn Reson Imaging 37(1), 156–163 (Jan 2013), http://dx.doi.org/10.1002/jmri.23781
8. Freiman, M., Perez-Rossello, J.M., Callahan, M.J., Voss, S.D., Ecklund, K., Mulkern, R.V., Warfield, S.K.: Reliable estimation of incoherent motion parametric maps from diffusion-weighted MRI using fusion bootstrap moves. Med Image Anal 17(3), 325–336 (Apr 2013), http://dx.doi.org/10.1016/j.media.2012.12.001
9. Freiman, M., Voss, S.D., Mulkern, R.V., Perez-Rossello, J.M., Callahan, M.J., Warfield, S.K.: In vivo assessment of optimal b-value range for perfusion-insensitive apparent diffusion coefficient imaging. Medical Physics 39, 4832 (2012)

10. Gloria, C., Li, Q., Xu, L., Zhang, W.: Differentiation of diffusion coefficients to distinguish malignant and benign tumor. J Xray Sci Technol 18(3), 235–49 (2010)
11. Klauss, M., Lemke, A., Grunberg, K., Simon, D., Re, T.J., Wente, M.N., Laun, F.B., Kauczor, H.U., Delorme, S., Grenacher, L., Stieltjes, B.: Intravoxel incoherent motion MRI for the differentiation between mass forming chronic pancreatitis and pancreatic carcinoma. Invest Radiol 46(1), 57–63 (2011)
12. Koh, D.M., Collins, D.J., Orton, M.R.: Intravoxel incoherent motion in body diffusion-weighted MRI: reality and challenges. AJR Am J Roentgenol 196(6), 1351–61 (2011)
13. Le Bihan, D.: Intravoxel incoherent motion perfusion MR imaging: a wake-up call. Radiology 249(3), 748–52 (2008)
14. Le Bihan, D., Breton, E., Lallemand, D., Aubin, M.L., Vignaud, J., Laval-Jeantet, M.: Separation of diffusion and perfusion in intravoxel incoherent motion MR imaging. Radiology 168(2), 497–505 (1988)
15. Lemke, A., Laun, F.B., Klauss, M., Re, T.J., Simon, D., Delorme, S., Schad, L.R., Stieltjes, B.: Differentiation of pancreas carcinoma from healthy pancreatic tissue using multiple b-values: comparison of apparent diffusion coefficient and intravoxel incoherent motion derived parameters. Invest Radiol 44(12), 769–75 (2009)
16. Lemke, A., Stieltjes, B., Schad, L.R., Laun, F.B.: Toward an optimal distribution of b values for intravoxel incoherent motion imaging. Magn Reson Imaging 29(6), 766–76 (2011)
17. Luciani, A., Vignaud, A., Cavet, M., Nhieu, J.T., Mallat, A., Ruel, L., Laurent, A., Deux, J.F., Brugieres, P., Rahmouni, A.: Liver cirrhosis: intravoxel incoherent motion MR imaging–pilot study. Radiology 249(3), 891–9 (2008)
18. Mulkern, R.V., Vajapeyam, S., Robertson, R.L., Caruso, P.A., Rivkin, M.J., Maier, S.E.: Biexponential apparent diffusion coefficient parametrization in adult vs newborn brain. Magn Reson Imaging 19(5), 659–68 (2001)
19. Patel, J., Sigmund, E.E., Rusinek, H., Oei, M., Babb, J.S., Taouli, B.: Diagnosis of cirrhosis with intravoxel incoherent motion diffusion MRI and dynamic contrast-enhanced MRI alone and in combination: preliminary experience. J Magn Reson Imaging 31(3), 589–600 (2010)
20. Re, T.J., Lemke, A., Klauss, M., Laun, F.B., Simon, D., Grunberg, K., Delorme, S., Grenacher, L., Manfredi, R., Mucelli, R.P., Stieltjes, B.: Enhancing pancreatic adenocarcinoma delineation in diffusion derived intravoxel incoherent motion f-maps through automatic vessel and duct segmentation. Magn Reson Med 66(5), 1327–32 (2011)
21. Sigmund, E.E., Cho, G.Y., Kim, S., Finn, M., Moccaldi, M., Jensen, J.H., Sodickson, D.K., Goldberg, J.D., Formenti, S., Moy, L.: Intravoxel incoherent motion imaging of tumor microenvironment in locally advanced breast cancer. Magn Reson Med 65(5), 1437–47 (2011)
22. Winkler, G.: Image Analysis, Random Fields and Dynamic Monte Carlo Methods. Springer, New York, 2nd edn. (2003)
23. Yamada, I., Aung, W., Himeno, Y., Nakagawa, T., Shibuya, H.: Diffusion coefficients in abdominal organs and hepatic lesions: evaluation with intravoxel incoherent motion echo-planar MR imaging. Radiology 210(3), 617–23 (1999)